

## STRUCTURE AND STRESSES IN NiCoFeCrMn HIGH-ENTROPY ALLOYS IRRADIATED WITH LOW-ENERGY HELIUM IONS

V.V. Uglov<sup>1</sup>), N.A. Stepanyuk<sup>1</sup>), S.V. Zlotski<sup>1</sup>), K. Jin<sup>2</sup>), A.M. Yaqoob<sup>3</sup>), D.V. Esipenko<sup>1</sup>)

<sup>1</sup>Belarusian State University,

4 Nezavisimosti Ave., 220030 Minsk, Belarus, uglov@bsu.by, nik.stepanjuk.99@mail.ru,  
zlotski@bsu.by, ya.alukard2014@yandex.by

<sup>2</sup>Beijing Institute of Technology,

№ 5 South Str., Zhongguancun, Haidian District, 100081 Beijing, China, jinke@bit.edu.cn

<sup>3</sup>Technology Innovation Institute,

9639 Abu Dhabi, Masdar City, United Arab Emirates, ali.yaqoob@tii.ae

NiCoCrFeMn and NiCoCrFe high-entropy alloys are formed by the method of arc melting and casting in a copper cell, followed by vacuum annealing at a temperature. Studies carried out by scanning electron microscopy and XRD analysis showed that the formed HEAs have a coarse-grained structure (80-100  $\mu\text{m}$ ) and are single-phase substitutional solid solutions with an fcc lattice. High-entropy alloys were irradiated at room temperature with He ions with the energy of 40 keV at fluences from  $3 \cdot 10^{17}$  to  $5 \cdot 10^{17}$   $\text{cm}^{-2}$ . It was found that irradiation with helium ions does not lead to erosion of the sample surface, as well as to the decomposition of NiCoCrFeMn and NiCoCrFe solid solutions. An increase in the root-mean-square deviation and tensile stresses in the samples under irradiation with helium ions is revealed. It was found that the most radiation-resistant system is NiCoCrFeMn.

**Keywords:** High-entropy alloys; helium ion irradiation; coarse-grained structure; single-phase solid solutions; root-mean-square deviation; initial stress.

### Introduction

Since the coining of the term High Entropy Alloys (HEA) in 2004 by Yeh [1], HEAs have attracted a lot of the scientific community's attention as a more defect resistant and more stable material under extreme conditions. High-entropy alloys are a type of concentrated single-phase solid-solution alloy. HEAs typically include four or more elements in approximately equiatomic ratios, with the components randomly organised on a face-centered cubic (FCC) or body-centered cubic (BCC) crystalline lattice [1]. When compared to more traditional, binary, solid-solution alloys, the lack of ordered elemental arrangement and the associated high configurational entropy in these alloys has been observed to yield improved resistance to radiation damage [2]. For example, radiation-induced segregation at grain boundaries was considerably reduced in FeNiMnCr HEAs as compared to irradiated typical austenitic FeCrNi alloys [3]. Other research groups [2] and [4-7] have also found that many different types of damaged HEAs exhibit exceptional phase stability and radiation resistance at moderate-to-high damage levels [8].

The irradiation response of HEAs and their ability to survive the neutron bombardment environment of future civil nuclear power plants are gaining attention. Face-centered cubic CrMnFeCoNi, commonly known as the Cantor alloy, was one of the earliest suggested HEAs, and the irradiation response of the Cantor alloy and its sub-systems is the subject of this research [8].

Utilising irradiation analogues (electrons, heavy ions, and He) to neutron bombardment, as well as simulations, advanced microstructural analysis, and property measurement, the Cantor alloy and its derivatives are shown to have encouraging irradiation resistance that, in many cases, outperforms more traditional dilute alloys with same elements [3], [7]. High phase stability and resistance to radiation-induced segregation, smaller size but higher density of dislocation loops, considerably reduced swelling extent, and enhanced resistance to He bubble development are all advantages.

### Materials and methods

Samples NiCoCrFeMn and NiCoCrFe were manufactured at the Beijing

Technological University by arc melting and casting in a copper cell, followed by vacuum annealing at a temperature of 1150°C for 24 h, cold rolling until the thickness is reduced by 85%, and final annealing at a temperature of 1150°C for 72 h (Fig. 1).

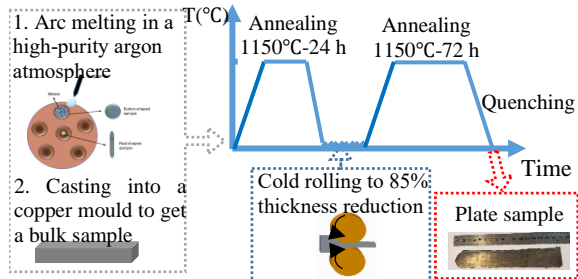


Fig. 1. High-entropy sample preparation scheme

Ion implantation of the HEAs was carried out using 40 keV  $\text{He}^{2+}$  ions at the DC-60 heavy ion accelerator of the Astana branch of the Institute of Nuclear Physics at the fluence from  $3.0 \cdot 10^{17}$  to  $5 \cdot 10^{17} \text{ cm}^{-2}$ . The implantation temperature was 300 K. The beam current was 200  $\mu\text{A}$ , and water cooling of the target substrate was used.

X-ray Diffraction (XRD) analysis was employed for structural identification using an Ultima IV Rigaku X-ray diffractometer operating in parallel configuration and equipped with  $\text{CuK}\alpha$  wavelength (0.15418 nm). In view of the structural features of the HEAs, the XRD spectra were obtained while the sample was rotating in the plane of its surface. The stresses in the HEAs were calculated by the  $\sin^2\psi$  method for the (220) plane.

The morphology of the HEAs surface was studied by the method of scanning electron microscopy (SEM) on plan-view specimens using a JEOL JSM-7500F Field Emission Scanning Electron Microscope.

## Results and discussion

The SEM method revealed that the obtained samples have a coarse-grained structure, the grain size for the CoCrFeMnNi sample was 100  $\mu\text{m}$ , and for the CoCrFeNi sample 80  $\mu\text{m}$ . The grains are regular in shape with hexagonal sections. Also on the surface, traces of twinning are clearly visible, introduced by mechanical processing of the samples during preparation, which can contribute to an

increase in the radiation resistance of these alloys by the presence of a drain of defects in the form of twin boundaries (Fig. 2a).

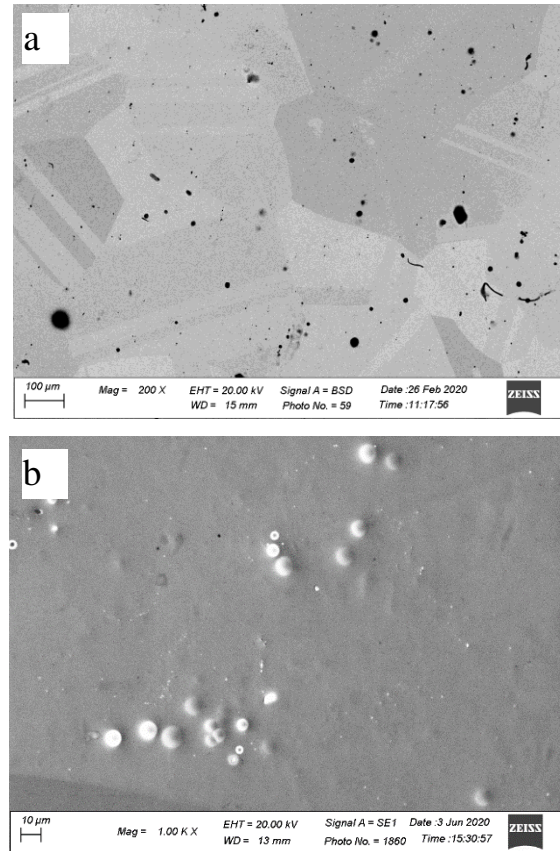


Fig. 2. SEM micrograph of an unirradiated NiCoCrFeMn HEA (a) and a Ni sample (b) irradiated with He (40 keV and  $3 \cdot 10^{17} \text{ cm}^{-2}$ ) ions

Figures 3, 4 show part of the XRD spectra of the initial NiCoCrFeMn and NiCoCrFe samples, respectively. Analysis of XRD spectra of the obtained samples revealed that they are single-phase substitutional solid solutions with an fcc lattice. The lattice parameter of the NiCoCrFeMn alloy is 0.359 nm, and that of the NiCoCrFe alloy is 0.357 nm.

The results of determining the internal stresses in the initial samples, calculated by the  $\sin^2\psi$  method for the diffraction peak (220), are presented in Table 1. As can be seen from the table, the compressive stress of -55 and -150 MPa are formed in the initial samples for NiCoCrFeMn and NiCoCrFe samples, respectively.

Before investigation of irradiated HEAs, calculations using SRIM program [9] were performed. SRIM calculations showed that

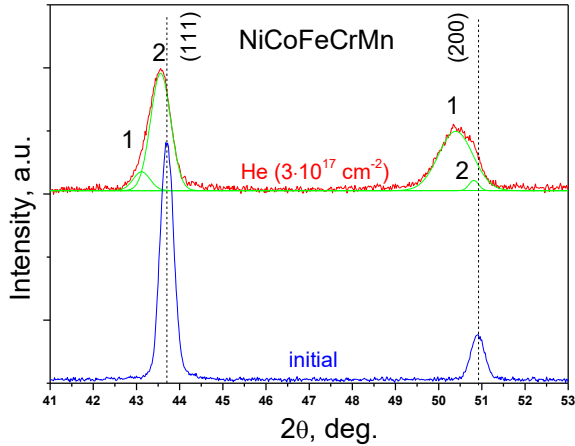


Fig. 3. XRD spectra of initial and irradiated by He (40 keV and  $3 \cdot 10^{17} \text{ cm}^{-2}$ ) ions NiCoFeCrMn HEAs obtained at an X-ray beam incidence angle of  $1^\circ$

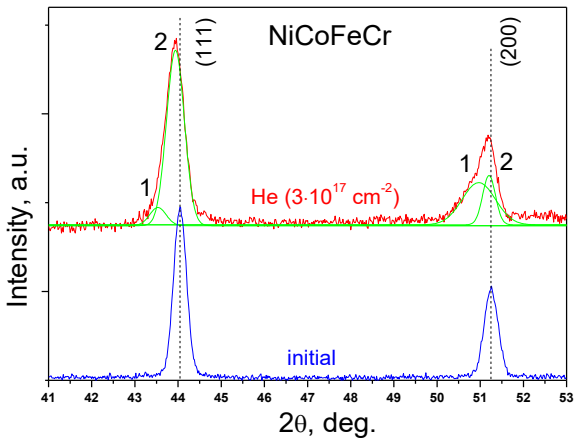


Fig. 4. XRD spectra of initial and irradiated with He (40 keV and  $3 \cdot 10^{17} \text{ cm}^{-2}$ ) ions NiCoFeCr HEAs obtained at an X-ray beam incidence angle of  $1^\circ$

the range of He is 147 and 144 nm for NiCoCrFeMn and NiCoCrFe systems, respectively (Table 1). The energy loss for all samples is about 225 eV/nm.

Table 1. Stress of initial and  $R_p$ , root-mean-square deviations, stress of HEAs irradiated with He (40 keV and  $3 \cdot 10^{17} \text{ cm}^{-2}$ ) ions

Samples	$R_p$ , nm	RMSD	Stress, MPa	
			initial	He irradiated
NiCoCrFeMn	147	1.16 (Peak 1)	-55	72
		0.94 (Peak 2)		
NiCoCrFe	144	0.83 (Peak 1)	-150	82
		0.63 (Peak 2)		

SEM studies of irradiated HEAs did not reveal radiation erosion of the sample surface, that is, no traces of blistering or flaking were found at a fluence of  $5 \cdot 10^{17} \text{ cm}^{-2}$ . In this case, for Ni samples obtained by the same method,

the formation of blisters with a diameter of 10  $\mu\text{m}$  was found already at a fluence of  $3 \cdot 10^{17} \text{ cm}^{-2}$  (Fig. 2b). The data obtained indicate a high radiation resistance of the HEAs surface to erosion after helium ions irradiation with a fluence of  $5 \cdot 10^{17} \text{ cm}^{-2}$ .

XRD spectra of the irradiated and initial samples were obtained at an angle of incidence of the X-ray beam of  $1^\circ$  (Fig. 3, 4), due to the small depth of implantation of helium ions (about 300 nm).

Analysis of XRD spectra of irradiated HEAs did not reveal the decomposition of solid solutions or the formation of new phases, which indicates a high radiation resistance of the structure of HEAs solid solutions.

It was found that irradiation with helium ions leads only to a shift of the diffraction peaks of NiCoCrFeMn and NiCoCrFe solid solutions to the region of smaller angles (an increase in the lattice parameter). At the same time, the asymmetry of the diffraction peaks (111) and (200) was revealed, which made it possible to approximate them and divide them into two peaks (Fig. 3). As can be seen from Figures 3 and 4, peaks 2 are characterized by a small displacement of the angular position in comparison with the diffraction peaks of unirradiated samples. While peaks 1 are significantly shifted to the region of smaller angles and broadened. This separation of the peaks can be interpreted according to the SRIM data. Peaks 2 correspond to diffraction from the region with a low concentration of implanted helium, and peaks 1 - from the region of the maximum concentration of helium. Thus, irradiation with helium ions leads to the formation of deformed regions with predominantly radiation defects (vacancies and interstitial atoms) - peaks 1 and implanted helium - peaks 2. In this case, helium implantation leads to an increase in macro- (shift of the diffraction peak) and microstresses (broadening of diffraction peak).

Calculations of root-mean-square deviations (RMSD) (stresses of the 3rd kind) are presented in Table 1. As can be seen from Table 1, the RMSD characterizing the disorder of the solid solution for 5 component HEAs is

higher than for 4 components. In this case, in the region of the maximum concentration of implanted helium, the RMSD increases.

The results of calculating internal stresses in HEAs irradiated with helium are given in Table 1. As can be seen from the table, irradiation with helium ions leads to a decrease in compressive stresses and an increase in tensile ones. In this case, the greatest change in the stress level was revealed for the NiCoCrFe system. The change in the level of internal stresses is caused by helium implantation and the formation of radiation defects. Therefore, we can conclude that the NiCoCrFeMn system is more radiation-resistant than the NiCoCrFe system.

### Conclusions

NiCoCrFeMn and NiCoCrFe high-entropy alloys are formed by the method of arc melting and casting in a copper cell, followed by vacuum annealing at a temperature.

It was revealed that the formed HEAs have a coarse-grained structure (80-100  $\mu\text{m}$ ) and are single-phase substitutional solid solutions with an fcc lattice.

The high radiation resistance of the surface microstructure and phase composition of the formed high-entropy alloys has been established.

An increase in root-mean-square deviations and tensile stresses in HEAs under irradiation with helium ions is revealed.

It was found that the most radiation-resistant system is NiCoCrFeMn.

### References

1. Structural Materials for Liquid Metal Cooled Fast Reactor Fuel Assemblies. *IAEA Nuclear Energy Series* 2012; NF-T-4.3 Operational Behaviour, Vienna: IAEA.
2. Amekura H. Shape elongation of embedded metal nanoparticles induced by irradiation with swift heavy ions/cluster ions. *IEEE Nanotechnology Materials and Devices Conference (NMDC)*. 2016; 1-2.
3. Feuerbacher M., Heidelmann M. and Thomas C. Hexagonal High-entropy Alloys. *Materials Research Letters* 2015; 3(1); 1-6.
4. Kim Y.-K., Yang S. and Lee K.-A. Superior Temperature-Dependent Mechanical Properties and Deformation Behavior of Equiatomic CoCrFeMnNi High-Entropy Alloy Additively Manufactured by Selective Laser Melting. *Scientific Report* 2020; 10, 8045: 1-13.
5. G. M. C., Yeh J.W., Liaw P.K. and Zhang Y. High-Entropy Alloys: Fundamentals and Applications, Springer, 2016.
6. Körmann F., Ikeda Y., Grabowsk B. and Sluiter M.H.F. Phonon broadening in high entropy alloys. *Computational Materials* 2017; (3): 1-9.
7. Miracle D. B., Miller J. D., Senkov O. N. and Woodward C. Exploration and Development of High Entropy Alloys for Structural Applications. *Entropy* 2014; (16): 494-525.
8. Q. W. J. L. C. T. L. Y. Y. Y. F. Ye. High-entropy alloy: challenges and prospects. *Materials Today* 2016; 19(6): 349-362.
9. <http://www.srim.org/>.